Average magnetic moments of pre-yrast high spin states in ^{166,165}Hf

L. Weissman, M. Hass, and C. Broude
Department of Particle Physics, The Weizmann Institute of Science, Rehovot, Israel 76100
(Received 11 August 1995)

The average magnetic moments of high spin states in Hf isotopes were determined in a transient field measurement at the 14 MV Koffler accelerator of the Weizmann Institute. The reaction ^{130}Te(^{40}Ca,xn)^{166,165}Hf at beam energies from 167 to 182.5 MeV was used to populate different high spin regions and provide the recoiling Hf nuclei with sufficient velocity to traverse the 2.9 mg/cm^2 Gd ferromagnetic layer. Standard double ratios and angular distributions for various low level transitions were measured to determine precession angles. These carry information regarding the average g factor of unobservable transitions at medium excitation. To obtain a more quantitative analysis regarding the time-decay history of the γ cascade, Monte Carlo simulations of the cascade were carried out. The significance of the results for understanding the single particle nature of these pre-yrast levels is discussed.

PACS number(s): 21.10.Ky, 23.20.En, 25.70.Gh, 27.70.+q

I. INTRODUCTION

The measurements of g factors play an important role in nuclear structure physics since these moments probe mostly the single particle degrees of freedom. In particular, measurements of magnetic moments of high spin levels are sensitive to the dramatic changes in nuclear structure which take place due to single particle alignment. As an example, the measurements of g factors of high spin states in ^{158}Dy, ^{238}U, and ^{238}Th using the transient field (TF) technique have unambiguously determined the role of neutron and proton alignment in the structure of the backbending region [1,2].

Hf belongs to the rare earth elements for which high spin states have been the subject of intensive research in recent years [3–5]. As in most rare earth isotopes, the nuclei of some Hf isotopes are deformed. As the deformation decreases with neutron number approaching magic number 82, the backbending curve associated with the interaction of the yrast ground band and the aligned band becomes more pronounced due to smaller interband interaction strength. The isotope ^{166}Hf, with 94 neutrons, lies at the beginning of this transitional region between the deformed and spherical shape; it exhibits backbending but not as sharp as for the lighter isotopes [5]. The purpose of this publication is to probe for similar phenomena of neutron (proton) alignment for pre-yrast levels at medium excitation via the determination of their average magnetic moments.

The transient field is the only method available for magnetic moment determination of such short lived nuclear states. This technique makes use of the large hyperfine interaction experienced by fast nuclei traversing a ferromagnetic material [6]. The first attempt to measure the magnetic moments of such levels in Hf isotopes by applying TF was carried out by Skaali *et al.* in 1975 [6]. The ferromagnetic foil used for these early experiments was thick, causing the recoils to stop inside the ferromagnet and experience the static hyperfine field in addition to the transient field. Also, the Lindhard-Winther theory [7] was used to interpret the results, contrary to standard recent parametrizations (see below). The small values of the g factors of pre-yrast levels which were obtained, 0.07(4) for ^{168}Hf and 0.14(4) for ^{172}Hf, must therefore be considered only as tentative. This experiment was reanalyzed later using a more realistic TF parametrization [8], yielding g factors of 0.16(8) and 0.31(7) for ^{168}Hf and ^{172}Hf, respectively. It is of much interest to measure magnetic moments of Hf isotopes, especially in the lighter transitional region, with better accuracy using the TF technique with a thin ferromagnetic layer and a nonmagnetic stopper.

II. EXPERIMENT

The reaction ^{130}Te(^{40}Ca,4n)^{166}Hf was used to populate high spin states in the ^{166}Hf nucleus. Measurements were carried out at beam energies of 167.5, 170, 175, 180, and 182.5 MeV (see below). The main features of the vacuum chamber and the target structure are presented in Fig. 1. A 2.9 mg/cm^2 gadolinium foil was prepared by rolling, followed by annealing in high vacuum. An off-line magnetization measurement yielded 89% of the saturation value for gadolinium at 100 K in an external field of 0.04 T (Fig. 2). A thin gold layer (500 μg/cm^2) was evaporated on one side of the gadolinium foil and this side was pressed onto a clean, thick 25 mg/cm^2 gold foil. The tellurium layer of 700 μg/cm^2 was evaporated on the other surface of the gadolinium foil. Simulation of the target assembly using the TRIM [9] code shows that about 95% of the recoils traverse the gadolinium ferromagnetic layer. The remaining 5% could experience also the static field of Hf in gadolinium but this effect is negligible compared to the transient-field precession. The magnetization of the three-layer target was measured before and after the ion beam bombardment to check for possible changes due to diffusion, alloying, and radiation damage. No change with respect to the initial magnetization was found.

The target was mounted on a thin layer of boron nitride, attached to a cryogenic copper cold finger. This arrangement provided good thermal contact and electrical isolation from the cryofinger for monitoring the current on the target. The external part of the cryofinger was immersed in a Dewar of liquid nitrogen. The temperature of the cooled target was measured by a thermocouple to be 85 K. The large cold

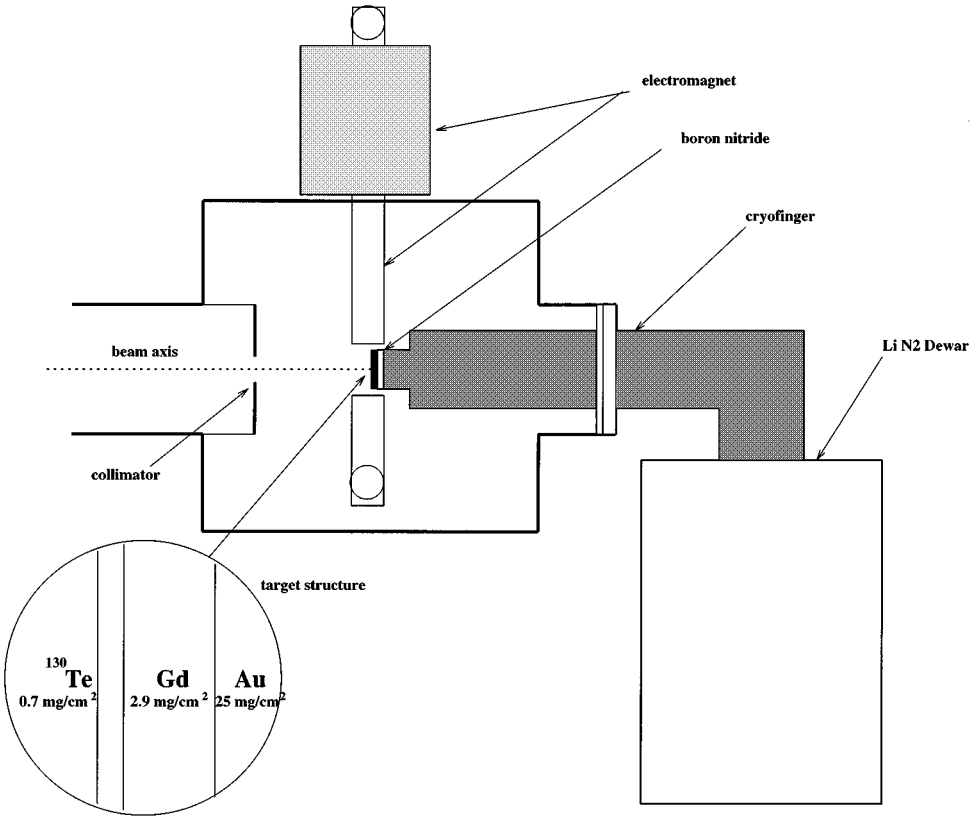

FIG. 1. The TF chamber and the target structure.

surface of the cryofinger served to improve the vacuum in the chamber (6×10^{-6} mtorr) and reduce the accumulation of cracked hydrocarbons on the target surface.

The ferromagnetic gadolinium was polarized by an external field of $B=0.06$ T in the 8 mm gap of an electromagnet. The direction of the polarizing field, and hence the transient field, was changed every 3 minutes by reversing the current in the electromagnet coil. This procedure allowed the double ratios (see below) to be constructed.

Decay γ rays were detected in four, 25%-efficient, Ge detectors surrounded by NaI anti-Compton shields. The detectors were placed in the horizontal plane, perpendicular to the direction of the magnetic field, at angles of large logarithmic slope of the angular distribution (55° and 125° with respect to the beam axis). Ten NaI detectors served as a multiplicity filter to reduce background in the Ge spectra due to contaminant lines from Coulomb excitation, activity of reaction products, and reactions with surface impurities. Two routing signals from the electromagnet controller unit indicated the two directions of the external field. Thus, two spectra corresponding to ''up'' and ''down'' field directions were generated for each detector, gated by the multiplicity requirement.

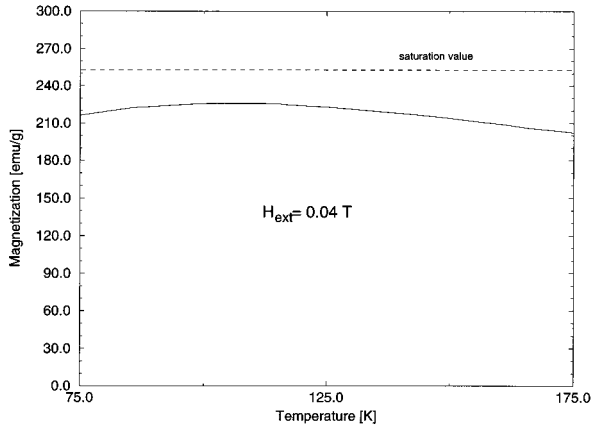

FIG. 2. Magnetization of the gadolinium foil in an external field of 0.04 T. The error bar of about 3% is mainly due to the uncertainty in the mass of the sample.

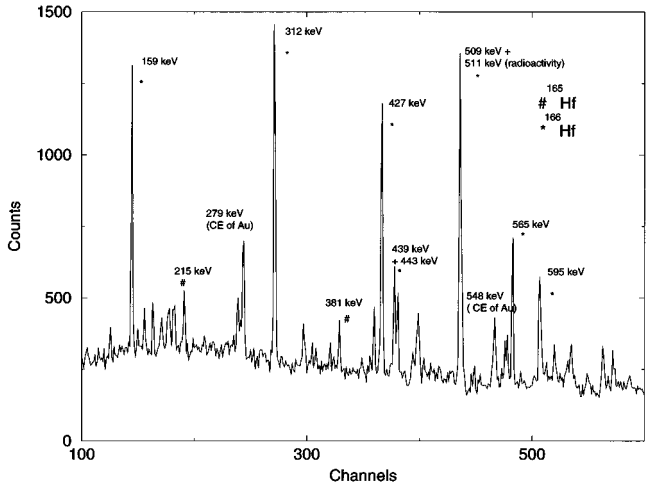

FIG. 3. γ spectrum from the ^{130}Te(^{40}Ca,4n)^{166}Hf at $E_{\text{beam}}=170$ MeV with a multiplicity condition of $M\geq2$. The two transitions from ^{165}Hf, 215 and 381 keV, are more prominent at the higher beam energies.

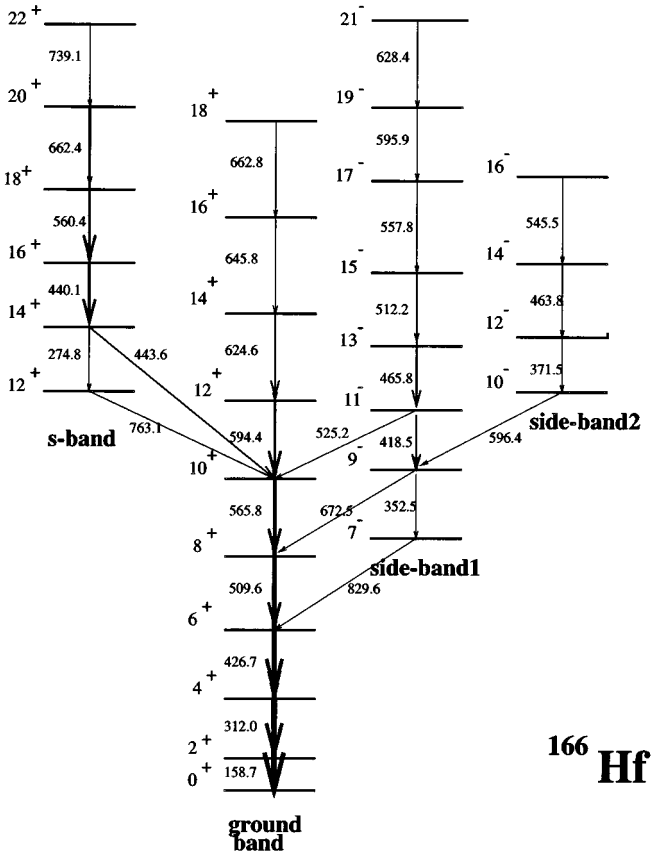

FIG. 4. The level scheme of ^{166}Hf (see, e.g., Ref. [5]).

III. RESULTS

A. The reaction spectrum

The average Ca ion current on the target was about 0.6 particle nA. The current had to be kept below 2 particle nA to avoid evaporation of the thin tellurium layer. A typical spectrum of the reaction under conditions of multiplicity $M \geqslant 2$ is shown in Fig. 3. The level scheme of ^{166}Hf is shown in Fig. 4 [5]. The high intensity of the $8^+ \rightarrow 6^+$ transition at 509.6 keV is due to contributions from the positron annihilation line at 511 keV, the $15^- \rightarrow 13^-$ transition of sideband 1 (sb1) and, at the higher energies, the $25/2^+ \rightarrow 21/2^+$ from ^{165}Hf. A higher multiplicity condition would be needed to further suppress the positron annihilation line. There are also some other unresolved doublet lines: $13^- \rightarrow 11^-$ (sb1) and $14^- \rightarrow 12^-$ (sb2), $13^- \rightarrow 11^-$ (sb1) and $14^- \rightarrow 12^-$ (sb2), $18^+ \rightarrow 16^+$ (sb) and $17^- \rightarrow 15^-$ (sb1), $18^+ \rightarrow 16^+$ (gb) and $20^+ \rightarrow 18^+$ (sb). The strong 279 and 548 keV transitions are due to Coulomb excitation of the gold backing which was not sufficiently suppressed by the $M \geqslant 2$ multiplicity condition. The two lowest ground state band transitions of ^{165}Hf [5] at 215 and 381 keV, respectively, from the ^{130}Te(^{40}Ca,5n) channel start to increase in intensity at energies higher than 170 MeV.

B. Angular distribution

The angular distribution was measured at the beam energy of 170 MeV at six angles 360°, 330°, 300°, 295°, 265°, and 235° for four ground band lines of ^{166}Hf: 159, 312, 427, and 509 keV.

TABLE I. The angular distribution coefficients A_2 and A_4 of ground band transitions in ^{166}Hf.

Transition	Energy (keV)	A_2	A_4
$2^+ \rightarrow 0^+$	159	0.38±0.06	0.07±0.07
$4^+ \rightarrow 2^+$	312	0.29±0.05	0.07±0.07
$6^+ \rightarrow 4^+$	427	0.25±0.05	-0.02±0.035
$8^+ \rightarrow 6^+$	509	0.18±0.06	-0.01±0.01

The extracted angular distribution function $W(\theta)$ was fitted by Legendre polynomials of second and fourth order:

$$W(\theta) = A_0[1 + A_2 P_2(\cos\theta) + A_4 P_4(\cos\theta)].$$

The results are summarized in Table I. The 509 keV transition exhibits a less anisotropic angular distribution due to the unresolved contribution from the positron annihilation radiation. Thus, angular distribution coefficients are averaged over the 159, 312, and 427 keV transitions, yielding $A_2 = 0.295 \pm 0.03$ and $A_4 = 0.01 \pm 0.03$. These coefficients yield a value of

$$S = \frac{1}{W(\theta)} \frac{dW(\theta)}{d\theta} = -0.41 \pm 0.02$$

for the logarithmic slope at 55° where the precession measurements were carried out. To verify that the angular distribution does not change significantly with beam energy, three short runs at different beam energies were performed, measuring the ratio of the line intensities, unnormalized by detector efficiency, between two detectors placed at 30° and 80° (Table II). The 30° to 80° ratio is a good measure of the angular distribution, and the slope S, of the lines used in the precession analysis and it is evident that this ratio is constant with energy within the errors. A very similar 30° to 80° ratio was also obtained for ^{165}Hf. Since the statistics for ^{165}Hf were limited, it is thus reasonable to use the same angular distribution coefficients, measured for ^{166}Hf, for the analysis of the precession data for this nucleus too.

C. Precession measurement

Standard double ratios were formed for backward (1,4) and forward (2,3) detectors:

$$\rho_{ij} = \left(\frac{N(\theta_i)\uparrow N(\theta_j)\downarrow}{N(\theta_i)\downarrow N(\theta_j)\uparrow} \right)^{1/2}$$

TABLE II. The raw $I_{30°}/I_{80°}$ ratio as function of beam energy. This ratio is unnormalized by detector efficiencies and serves to demonstrate the constancy, within the quoted errors, of the angular distribution.

Beam energy (MeV)	$I_{30°}/I_{80°}$ ^{166}Hf (312 + 426 keV)	$I_{30°}/I_{80°}$ ^{165}Hf (381 keV)
170	1.87±0.06	1.64±0.15
175	1.84±0.06	1.97±0.11
180	1.92±0.04	1.92±0.06

TABLE III. The precession of individual transitions for $E_{\text{beam}} = 170$ MeV.

Transition	Energy (keV)	$\epsilon \times 10^{-3}$
$2^+ \rightarrow 0^+$	159	8.3 ± 3.8
$4^+ \rightarrow 2^+$	312	10.1 ± 3.1
$6^+ \rightarrow 4^+$	427	10.0 ± 3.4
$10^+ \rightarrow 8^+$	565	10.3 ± 6.8
$12^+ \rightarrow 10^+$	595	4.7 ± 7.1
$14^+ \rightarrow 12^+$ and $16^+ \rightarrow 14^+$	439, 443	11.7 ± 6.8
$11^- \rightarrow 9^-$	418	8.2 ± 8.5
$13^- \rightarrow 11^-$	465	15.0 ± 8.1

where $N(\theta_i)\uparrow, N(\theta_i)\downarrow$ are the γ counts in detector i with the external field in the "up" and "down" directions, respectively. The double ratios do not depend on the detector efficiency or beam intensity fluctuations. Calculating the average double ratio

$$\rho = \left(\frac{\rho_{23}}{\rho_{14}}\right)^{1/2}$$

one can determine the angular precession $\Delta\theta$ by

$$\Delta\theta = S^{-1}\epsilon$$

where

$$\epsilon = \frac{\rho - 1}{\rho + 1}$$

is the precession effect and S is the logarithmic slope. The double ratios ρ_{13} and ρ_{24} are expected to be equal to unity and serve as consistency checks. A g factor is deduced from the measured angular precession angle $\Delta\theta$ using the Chalk River TF parametrization [8,10]:

$$B(v,Z) = 29Zv/v_0 \exp(-0.135v/v_0)[T]$$

where v_0 is Bohr velocity ($v_0 = \alpha c$) and Z is the atomic number of the recoiling nucleus. The uncertainty in the TF parametrization is of the order of 10%. The use of the alternative Rutgers parametrization [10] did not affect the extracted precession angles to any significant degree. The corresponding precession angle in such a field is

$$\Delta\theta = 1.487(gA/\rho c)\int_{v_{\text{in}}}^{v_{\text{out}}} B(v,Z)(dE/dx)^{-1}dv$$

where dE/dx is the stopping power (in MeV mg^{-1}cm^2) in gadolinium, ρ (in g/cm^3) is the density of gadolinium, A is the atomic mass, c is the speed of light, and B is in units of tesla. v_{in} and v_{out} are the entrance and exit velocities, respectively, of the Hf nuclei in the gadolinium layer.

The double ratios $\rho = (\rho_{23}/\rho_{14})^{1/2}$ of the individual lines were measured at several beam energies. As an example, we present here the results for ^{166}Hf transitions at the beam energy 170 MeV (Table III). The $8^+ \rightarrow 6^+$ 509 keV transition is not included because of the annihilation radiation contribution and interference from the $25/2^+ \rightarrow 21/2^+$ 509 keV transition in the ^{165}Hf isotope. The accuracy in the precession data for the individual transitions is marginal, but the statistical sum of all lines has adequate accuracy. We obtain

$$\epsilon = 0.01005 \pm 0.00155$$

and the consistency checks yield

$$\rho_{13} = 0.996 \pm 0.004, \quad \rho_{24} = 0.9965 \pm 0.004.$$

Measurements with a warm target (no magnetization) were carried out periodically during the experiment and yielded double ratios consistent with unity, as expected.

TABLE IV. Results of g factor measurements of ^{165,166}Hf.

E_{beam} (MeV)	ϵ 10^{-3}	$\Delta\theta$ (mrad)	g
^{166}Hf			
167.5	10.6±1.3	−25.9±3.2	0.23(3)(2)
170	9.6±1.7	−23.4±4.1	0.21(4)(2)
175	7.6±0.9	−18.5±2.2	0.16(2)(2)
180	9.6±1.4	−23.4±3.4	0.21(3)(2)
182.5	10.1±1.6	−24.6±3.9	0.22(3)(2)
^{165}Hf			
175	5.8±2.7	−14.1±6.6	0.13(6)(1)
180	7.6±2.2	−18.5±5.4	0.17(5)(2)
182.5	5.4±2.4	−13.2±5.9	0.12(5)(1)

The results of similar measurements for ^{165,166}Hf at various beam energies are presented in Table IV. The quoted errors on the g factors are the statistical and systematic errors, respectively. It is important to note that the comparison of different beam energies (see below) does not depend on the systematic errors associated with the TF parametrization.

IV. DISCUSSION

A. Monte Carlo simulations

The TF precession carries information regarding average magnetic moments of the ensemble of states which are populated within the narrow time window defined by the passage of the recoiling nuclei through the gadolinium layer. Monte Carlo simulations were carried out to map the decay cascade [11,12]. The first step in this procedure is an estimate of the means and widths of the nuclear spin and energy distributions after the evaporation of the last particle. The average spin of the compound nucleus after the reaction was estimated using a classical black sphere model, taking into account the energy loss of the beam inside the target. The evaporated neutrons carry away, on average, one half unit of angular momentum. The initial excitation energy was taken just below the neutron separation energy, about 6 MeV above the yrast line at the entry spin value. The γ cascade proceeds from the entry distribution, governed by competition between statistical $E1$'s and collective $E2$'s. The $E1$ decay is determined by the level density parameter and the γ-ray strength function. The first part of the statistical $E1$ cascade takes place before the recoiling nuclei reach the ferromagnetic layer as the mean time of the last $E1$ γ ray before the first $E2$ γ ray is about 40 fs. The $E2$ decay is determined by a moment of inertia $\mathcal{J} \approx 73\hbar^2$ MeV^{-1} and a quadrupole

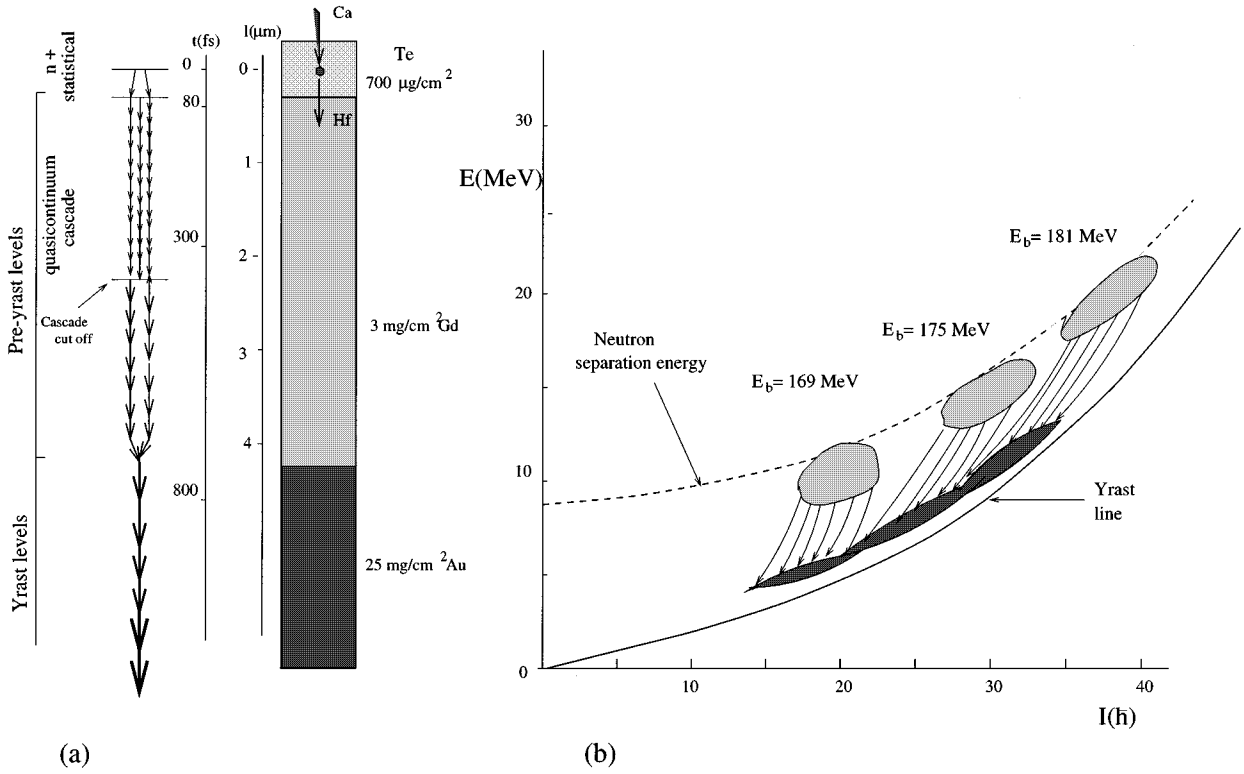

FIG. 5. (a) A schematic illustration of the γ-decay history and recoil kinematics inside the target at $E_{\text{beam}}=170$ MeV. (b) The pictorial illustration of the Monte Carlo simulations for three beam energies; for each case the entry distribution and region of the quasicontinuum cascade termination are sketched (see text).

moment $Q \approx 6\ e$b [13]. The quasicontinuum cascade is terminated when the excitation energy above the yrast line is less than $U_0 \approx 1.5$ MeV, where the discrete level structure first appears and the quasicontinuum approach is no longer valid [14]. The mean time until the termination of the quasicontinuum cascade is about 300 fs. The connection between the decay history of the γ cascade and the recoil kinematics in the target is sketched schematically in Fig. 5. The results of simulations are given in Table V. The nuclear spin and excitation energy inside the gadolinium layer are denoted as I_{Gd} and E_{Gd}. It is important to note that the Monte Carlo calculations depend necessarily on the assumptions of the model and on the values of the parameters above and are therefore meant only to guide the examination and discussion of the experimental results.

B. Conclusion

The magnetic moments of a ''warm'' nucleus at an excitation energy of about 1–1.5 MeV above the yrast line were measured at a number of beam energies, corresponding to various excitation energies in the final nucleus. The results of the measurements are shown in Fig. 6. The reduction of the g factors in ^{166}Hf compared with the collective rotation g factors of 2^+ levels which range from 0.27 to 0.35 for rare earth nuclei [15] indicates an appreciable contribution of aligned neutrons, for example from the $i_{13/2}$ orbital for which $g_{i_{13/2}} =$

TABLE V. Results of Monte Carlo simulations for ^{166}Hf.

E_{beam} (MeV)	$\langle I_{\text{entry}} \rangle$ ($\hbar$)	$\langle E_{\text{entry}} \rangle$ (MeV)	I_{Gd} ($\hbar$)	E_{Gd} (MeV)
169	19	10.9	18–15	6–4
175	29	14.6	27–22	8.5–6.5
181	38	19.4	35–27	11.5–8

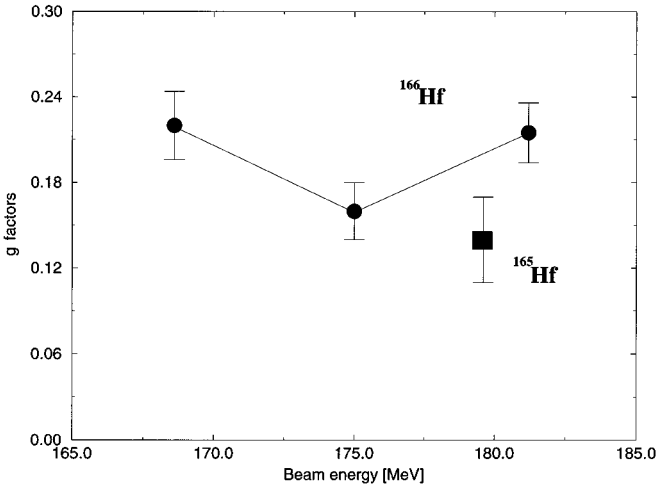

FIG. 6. Measured g factors of ^{165,166}Hf. For ^{166}Hf, we present results at three energies: the average of $E_{\text{beam}} = 167.5$ and 170 MeV, 175 MeV, and the average of $E_{\text{beam}} = 180$ and 182.5 MeV, respectively. The line connecting the ^{166}Hf points is to guide the eye. The result for ^{165}Hf is an average of the highest three energies. The plotted errors are statistical only as the systematic error is common to all points.

-0.16 [15] or from other $j=l+1/2$ orbital with similar g factors. In particular, the data suggest a significant reduction of the g factor at $E_{\mathrm{beam}} = 175$ MeV. As smaller g factors are associated with an enhanced neutron contribution to the total spin of the level(s) under study ($22-27\hbar$, see Table V and Figs. 5 and 6), this observation calls for additional experimental and theoretical work in order to achieve a better understanding of the systematics of neutron and/or proton alignment in this spin region. Similar experiments on lighter Hf isotopes, with the more pronounced back bending in their yrast bands, are currently in progress.

The results for ^{165}Hf do not allow comparison between the various beam energies due to poor statistics and we quote only an average for the three highest energies. The significantly smaller g factor of ^{165}Hf could be simply explained by the existence of an additional unpaired neutron as compared to the ^{166}Hf isotope. A recent experiment [16] with the EUROGAM-I array on ^{193}Hg yielded similar results for several bands in this odd-neutron nucleus, also demonstrating the role of the unpaired $i_{13/2}$ neutron in the structure of high spin levels at medium excitation.

There are several previous measurements of average magnetic moments of high spin levels in this mass region [12,16–20]. In general, lower g factors, indicating enhanced neutron contribution to the total spin for medium and high spin states, are exhibited in those studies as well. This trend seems to form a rather general rule and as such calls for a better theoretical understanding of this phenomenon.

ACKNOWLEDGMENTS

We wish to express our gratitude to Mr. Leo Sapir for his skillful target preparation. We would like to thank Professor S. Reich and Dr. T. Godin for measuring the magnetizations of the gadolinium foils and Dr. T. Lauritsen for his assistance in running the Monte Carlo code. We thank Mr. Igal Shahar and the Koffler accelerator crew for their help during the experiment. This work was supported in part by the Minerva Foundation.

[1] G. Seiler-Clark, D. Pelte, H. Emling, A. Balanda, H. Grein, E. Grosse, R. Kulessa, D. Schwalm, M. Hass, G. Kumbartzki, and K.H. Speidel, Nucl. Phys. **A399**, 211 (1983).

[2] O. Häusser, H. Gräf, L. Grodzins, E. Jaeschke, V. Metag, D. Habs, D. Pelte, H. Emling, E. Grosse, R. Kulessa, D. Schwalm, R.S. Simon, and J. Keinonen, Phys. Rev. Lett. **48**, 383 (1982).

[3] Y.K. Agarwal, J. Recht, H. Hübel, M. Guttormsen, D.J. Decman, H. Kluge, K.H. Maier, J. Dudek, and W. Nazarewicz, Nucl. Phys. **A399**, 199 (1983).

[4] M. Neffgen, E.M. Beck, H. Hübel, J.C. Bacelar, M.A. Deleplanque, R.M. Diamond, F.S. Stephens, and J.E. Draper, Z. Phys. A **344**, 235 (1993).

[5] K.P. Blume, H. Hübel, M. Murzel, J. Recht, K. Theine, H. Kluge, A. Kuhnert, K.H. Maier, A. Maj, M. Guttormsen, and A.P. De Lima, Nucl. Phys. **A464**, 445 (1987).

[6] B. Skaali, R. Kalish, J. Eriksen, and B. Herskind, Nucl. Phys. **A238**, 159 (1975).

[7] J. Lindhard and A. Winther, Nucl. Phys. **A166**, 413 (1971).

[8] O.F. Häusser, N. Rud, H.R. Andrews, D. Ward, J. Keinonen, P. Skensved, R. Nicole, and P. Taras, Chalk-River Report No. PR-P-126 AECL-7055, 1980, p. 20; O.F. Häusser, H.R. Andrews, D. Horn, M.A. Lone, P. Taras, P. Skensved, R.M. Diamond, M.A. Delepanque, E.L. Dines, A.O. Macchiavelli, and F.S. Stephens, Nucl. Phys. **A412**, 141 (1984).

[9] J.F. Ziegler, J.P. Biersack, and U. Littmark, in *The Stopping and Range of Ions in Solids* (Pergamon Press, New York, 1985); the calculations were carried out with the TRIM '91 version.

[10] N. Benczer-Koller, M. Hass, and J. Sak, Annu. Rev. Nucl. Part. Sci. **30**, 53 (1980).

[11] R. Holzmann, I. Ahmad, B.K. Dichter, H. Emling, R.V.F. Janssens, T.L. Khoo, W.C. Ma, M.W. Drigert, U. Garg, D.C. Radford, P.J. Daly, Z. Grabowski, H. Helppi, M. Quader, and W. Trzaska, Phys. Lett. B **195**, 321 (1987).

[12] M. Hass, N. Benczer-Koller, G. Kumbartzki, T. Lauritsen, T.L. Khoo, I. Ahmad, M.P. Carpenter, R.V.F. Janssens, E.F. Moore, F.L.H. Wolfs, Ph. Benet, and K. Beard, Phys. Rev. C **44**, 1397 (1991).

[13] B. Bochev, S. Ivlev, R. Kalpakchieva, S.A. Karaian, T. Kutsarova, E. Nadjakov, and Ts. Vencova, Nucl. Phys. **A282**, 159 (1977).

[14] T. Lauritsen (private communication).

[15] P. Raghavan, At. Data Nucl. Data Tables **42**, 189 (1989).

[16] N. Benczer-Koller, C. Broude, R.M. Clark, M. Hass, M. Joyce, G. Kumbartzki, N. Matt, H.R. Mayer, J. Sharpey-Schafer, and L. Weissman, in Proceedings of the 5th International Spring Conference on Nuclear Physics, Ravello, 1995.

[17] N. Rud, D. Ward, H.R. Andrews, O. Häusser, P. Taras, J. Kiekonen, M. Nieman, R.M. Diamond, and F.S. Stephens, Phys. Lett. **101B**, 35 (1981).

[18] O. Häusser, D. Ward, H.R. Andrews, P. Taras, B. Haas, M.A. Deleplanque, R.M. Diamond, E.L. Dines, A.O. Machiaveli, and C.V. Stager, Phys. Lett. **144B**, 341 (1984).

[19] E. Lubkiewicz, H. Emling, H. Grein, R. Kulessa, R.S. Simon, H. J. Wollersheim, Ch. Ender, J. Gerl, D. Habs, and D. Schwalm, Z. Phys. A **335**, 369 (1990).

[20] U. Birkental, A.P. Byrne, S. Heppner, H. Hübel, W. Schmitz, P. Fallon, F.D. Forsyth, J.W. Roberts, H. Kluge, F. Lubkiewicz, and G. Goldring, Nucl. Phys. **A555**, 643 (1993).